



## Communication

# Combined nanosuspensions from two natural active ingredients for cancer therapy with reduced side effects

Yonghui Qiao<sup>a</sup>, Zhihao Wei<sup>b</sup>, Tingting Qin<sup>c</sup>, Rufeng Song<sup>b</sup>, Zhiqiang Yu<sup>c</sup>, Qi Yuan<sup>b</sup>, Juan Du<sup>d</sup>, Qingbing Zeng<sup>c,\*</sup>, Lanlan Zong<sup>b,\*</sup>, Shaofeng Duan<sup>b,\*</sup>, Xiaohui Pu<sup>b,\*</sup>

<sup>a</sup> Henan University of Chinese Medicine, Zhengzhou 450046, China

<sup>b</sup> Institute of Pharmacy, School of Pharmacy, Henan University, Kaifeng 475004, China

<sup>c</sup> School of Pharmaceutics Sciences, Southern Medical University, Guangzhou 510515, China

<sup>d</sup> Department of Pharmacy, The Affiliated Cancer Hospital of Zhengzhou University, Zhengzhou 450003, China

## ARTICLE INFO

## Article history:

Received 12 January 2021

Received in revised form 17 March 2021

Accepted 19 March 2021

Available online 22 March 2021

## Keywords:

Combination therapy

Multidrug resistance

Nanosuspensions

Antitumor activity

Immunomodulatory

## ABSTRACT

Tumor drug resistance and systemic side effects of chemotherapeutic drugs are the main reasons for the failure of cancer treatment. In recent years, it was found that some natural active ingredients can reverse MDR and regulate body immunity to enhance the efficacy and reduce toxicity of chemotherapeutic drugs. In this paper, a new nanosuspensions, HCPT and QUR hybrid nanosuspensions (HQ-NPs), was prepared by the microprecipitation-high pressure homogenization method to reverse tumor drug resistance, reduce toxicity, and increase therapeutic efficacy. The *in vitro* investigation results showed that HQ-NPs had a unique shape (particle size was about  $216.3 \pm 5.9$  nm), changed crystalline, and different dissolution rates compared with HCPT-NPs and QUR-NPs, which is attributed to the strong intermolecular forces between HCPT and QUR as indicated by the results of the molecule dock. It was verified that the HQ-NPs could double the retention of HCPT in cells and enhance the cytotoxicity to A549/PTX cells *in vitro* tests compared with HCPT-NPs. We also found that HQ-NPs can significantly enhance the accumulation of HCPT in tumor sites, improve the antitumor activity of HCPT, and protect the immune organs and other normal tissues ( $P < 0.01$ ), compared with HCPT-NPs. Therefore, hybrid nanosuspensions can offer promising potential as the drug delivery system for HCPT and QUR to increase the therapeutic efficacy and reduce the toxicity of HCPT.

© 2021 Chinese Chemical Society and Institute of Materia Medica, Chinese Academy of Medical Sciences. Published by Elsevier B.V. All rights reserved.

Cancer is still a major threat to human health. To date, pharmaceutical therapy has become one of the indispensable means for comprehensive treatment of cancer. However, multidrug resistance (MDR) is the main obstacle of tumor chemotherapy, which is the most common and intractable issue for chemotherapy [1,2]. Due to the complex and diverse mechanisms of MDR, such as enhancing drug efflux, increasing DNA damage repair, reducing apoptosis, improving autophagy, changing drug metabolism [3,4], chemotherapy with a single drug is often ineffective. To overcome these problems, the combined therapy of multiple drugs catches scholars' interests, such as the combination of antitumor drugs with efflux protein inhibitors [5], regulators of multidrug resistance-related genes [6], and immunotherapy agents [7]. Combined therapy can minimize side effects, produce

synergistic or additive effects [8], and maximize the therapeutic effect and reverse MDR [9]. Several combined drug nanoparticles have come out in the past decade, such as paclitaxel/disulfiram (PTX/DSF) co-loaded micelles [10] and paclitaxel/magnetic nanoparticles/quantum dots encapsulated by biotin-poly(ethylene glycol)-poly(curcumin-dithio dipropionic acid) (PTX/MNPs/QDs@Biotin-PEG-PCDA) [11].

Hydroxycamptothecin (HCPT) is an indole alkaloid extracted from *Camptotheca acuminata*, which is a deciduous plant of *Davidia involucreta* endemic to China [12,13]. It is the most powerful anti-cancer compound of the monomers isolated from *Camptotheca acuminata* [14] and clinically used plant anticancer drug after paclitaxel [15]. However, HCPT is the substrate of a drug efflux protein, has a poorly soluble lactone ring and is commonly used in its carboxylate form in the clinic, which is highly toxic and has low activity [16]. Quercetin (QUR) is a natural flavonoid compound, which widely exists in various traditional Chinese medicines, fruits, and vegetables, such as berry, onion, tea and apple. It has extensive biological activities, such as anti-

\* Corresponding authors.

E-mail addresses: [zengqb@smu.edu.cn](mailto:zengqb@smu.edu.cn) (Q. Zeng), [lanlan19890321@126.com](mailto:lanlan19890321@126.com) (L. Zong), [dsf\\_2007@163.com](mailto:dsf_2007@163.com) (S. Duan), [pgh425@163.com](mailto:pgh425@163.com) (X. Pu).

inflammatory, anti-microbial, immunomodulatory, and anti-cancer effects [17]. It can also reverse MDR by downregulating the expression of P-gp, BCRP, MRP1, and so on, and inhibit the efflux of chemotherapy drugs [18,19]. It has been reported that QUR, as a potential chemical sensitizer, can inhibit the expression of mutant p53 and P-gp, and promote apoptosis [20]. Some studies also showed that it could produce a synergistic effect with several first-line chemotherapy drugs, such as Doxorubicin (DOX) [21] and PTX [22].

Nanosuspensions are widely favored as a matured nano-drug technology. They are submicron colloid dispersion systems formed by dispersing pure drug particles in water with a small amount of surfactant or polymer as the stabilizer. They have advantages of high drug loading, high chemical stability, good biosafety, and wide application for the “grease ball” and “brick dust” compounds, such as hydroxycamptothecin, nimodipine, quercetin [23–26]. Benefiting from the rapid development of biomaterials and nanotechnology, new nanotechnology is emerging in nano-drug delivery systems [27–31]. Hybrid nanocrystals have attracted more and more attention in recent years, especially in biomedical diagnosis, drug therapy and the study of the fate of drug nanocrystals [32,33]. However, so far, the hybrid nanocrystals of the two active molecules have been rarely reported.

Therefore, in the present study, we combined the anti-MDR and immunomodulatory effect of QUR with the anti-tumor effect of HCPT to prepare a hybrid nanosuspension (HQ-NPs) with high efficiency, low toxicity, and enhanced immunity, to achieve the purpose of synergism and reduced toxicity, as shown in Scheme 1. First, an amphiphilic triblock copolymer, poly(benzyl L-aspartate)-poly(ethylene glycol)-poly(benzyl L-aspartate) (PEG-(PBLA)<sub>2</sub>), was synthesized by ring-opening polymerization method (Fig. 1). In Fig. 1, the absorption peaks at  $\delta$  3.51 and  $\delta$  8.14 were the chemical shifts of H atom in  $-\text{CH}_2-$  (a) and H atom in  $-\text{NH}-$  (b) of poly(benzyl L-aspartate). The chemical shifts of H atom in  $-\text{CH}-$  (c) and in  $-\text{CH}_2-$  (d), H atom in  $-\text{CH}_2-$  (e) of benzyl group and in benzene ring (f) were  $\delta$  4.61, 2.81, 5.04, 7.30. As shown in the infrared spectra of the product (Fig. S1 in Supporting information),  $1660\text{ cm}^{-1}$  and  $1545\text{ cm}^{-1}$  were the characteristic absorption peaks of the carbonyl group in amide bond and the combined characteristic peaks of N—H bending vibration and C—N stretching vibration, respectively. Also, the characteristic absorbance from carbonyl groups in the anhydride bond and amide at  $1858\text{ cm}^{-1}$  and  $1793\text{ cm}^{-1}$  disappeared in the infrared spectra of the product. The above results indicated that PEG-(PBLA)<sub>2</sub> was successfully synthesized [23,34]. Subsequently, a hybrid nanosuspension was formulated by the microprecipitation-high pressure homogenization method using PEG-(PBLA)<sub>2</sub> as a stabilizer, which contains an

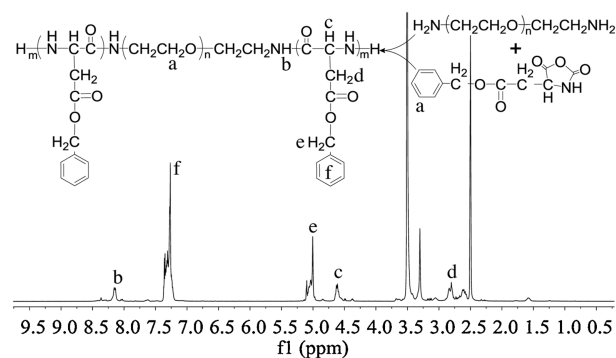
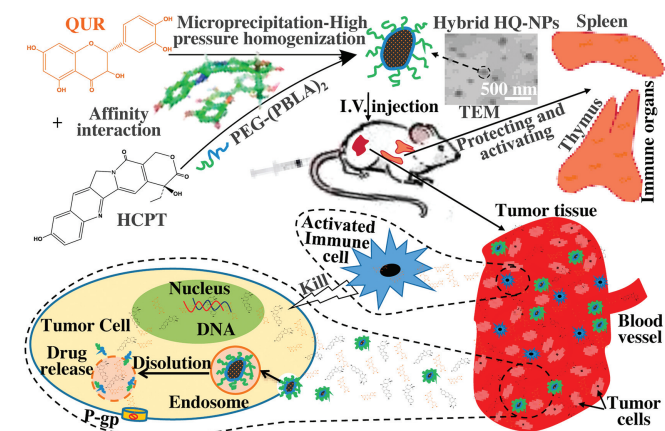


Fig. 1. The synthesis route and <sup>1</sup>H NMR spectrum (DMSO-*d*<sub>6</sub>) of PEG-(PBLA)<sub>2</sub>.

optimal combination ratio of two drugs (Q:H = 2:3, which is from the cytotoxicity data against A549/PTX cells showed in Fig. S2 in Supporting information). In this study, HCPT nanosuspension (HCPT-NPs) and QUR nanosuspension (QUR-NPs) were used as controls. As shown in Table 1 and Fig. 2A, the particle size, PDI and zeta potential across HCPT-NPs, QUR-NPs, and HQ-NPs formulations have no significant difference, and the size distributions were relatively uniform. And, the shape of QUR-NPs, HCPT-NPs, and HQ-NPs was spherical, rodlike, and quasi-spherical, respectively. The morphology of HQ-NPs was different from that of HCPT-NPs and QUR-NPs, which indicated the heterozygous nanoparticles were formed in HQ-NPs. The differences in the morphology may be attributed to the different crystal state of the two drugs in the three nanosuspensions [35].

To investigate the crystal state of the two drugs in the three nanosuspensions, differential scanning calorimetry (DSC) and X-ray powder diffraction (XRPD) analysis were carried out. As shown in Fig. S3A (Supporting information), compared with that of raw HCPT, one endo-thermic peak of HCPT shifted from  $281.82\text{ }^{\circ}\text{C}$  to  $275.13\text{ }^{\circ}\text{C}$  in the DSC spectra of HCPT-NPs, and the other two endothermic peaks disappeared. One exothermic peak of HCPT shifted from  $343.57\text{ }^{\circ}\text{C}$  to  $308.25\text{ }^{\circ}\text{C}$ , and the exothermic peak at  $126.69\text{ }^{\circ}\text{C}$  disappeared. In the DSC spectra of HQ-NPs, there were only exothermic peaks from stabilizers at  $187.52\text{ }^{\circ}\text{C}$  and an endothermic peak of HCPT at  $266.23\text{ }^{\circ}\text{C}$ , while other endothermic peaks disappeared. There was no obvious characteristic peak of QUR in the DSC spectra of QUR-NPs and HQ-NPs. These results indicated that the crystal phase transition of HCPT and QUR may occur during the formation of nanosuspensions, and the crystal form of HCPT in HQ-NPs may be different from that in HCPT-NPs [36]. Fig. S3B (Supporting information) shows that there are still some weak diffraction peaks of HCPT in the diffraction spectra of HCPT-NPs and HQ-NPs, while the diffraction peaks at  $15^{\circ}$ – $25^{\circ}$  disappeared. Comparing the diffraction pattern of QUR-NPs and raw QUR, the diffraction peaks of QUR was different in peak position and intensity, indicating that the crystal form of QUR in QUR-NPs had changed. There was no diffraction characteristic peak of QUR in the diffraction pattern of HQ-NPs, indicating that QUR might exist in the amorphous form in HQ-NPs. These results indicated that the formation process of nanosuspensions affected the physical states of the two drugs and that heterozygosity between the two drugs in HQ-NPs may occur due to assumed



Scheme 1. The formation and anti-tumor mechanisms of hybrid nanosuspensions.

Table 1  
Particle size and PDI of three nanosuspensions (*n* = 3).

Sample	Particle size (nm)	PDI	Zeta potential (mV)
HCPT-NPs	198.4 ± 6.45	0.209 ± 0.024	−19.40
QUR-NPs	222.5 ± 7.64	0.193 ± 0.060	−18.30
HQ-NPs	216.3 ± 5.93	0.197 ± 0.035	−14.20

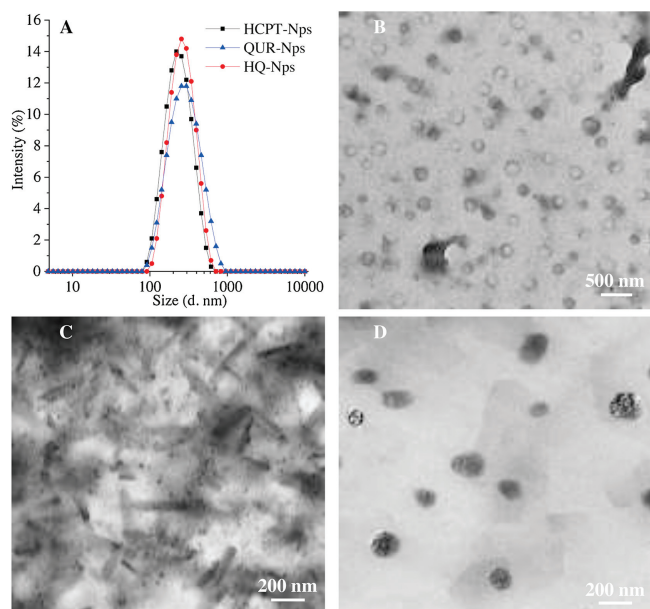


**Fig. 2.** The size distribution (A) and TEM images of QUR-NPs (B), HCPT-NPs (C), and HQ-NPs (D).

intermolecular forces between HCPT and QUR molecules [23]. To verify this assumption, MD was carried out to predicate the complexes between two molecules. The interaction strength between two molecules was evaluated using the binding energy. The binding energy of various molecule pair was listed in Table S1 (Supporting information). The binding affinities were stronger with the reduction of the binding energy. Therefore, a stable aggregate (or crystal) may be formed between molecules with strong binding affinity, which would impede the dissolution of the drug molecules. The conformations simulated by MD using the lower binding energy of  $-3.63$  suggest that the planar structure of HCPT and QUR have strong  $\pi$ - $\pi$  stacking and hydrophobic interactions due to their aromatic conjugation (Fig. S4 in Supporting information). Based on the confirmation of the different binding energy, the HQ-NPs crystal form differs from

QUR-NPs and HCPT-NPs, which could give a reason why the shape of HQ-NPs in TEM images was different from those of QUR-NPs and HCPT-NPs.

Stability is one of the most important properties for nanosuspensions. In present study, several stability tests were implemented. As shown in Fig. 3A, the particle size of the three nanosuspensions changed little when stored at  $4^{\circ}\text{C}$  vs. room temperature for one month, which indicated that the three nanosuspensions had good storage stability. Also, the transmittance of all formulations showed little increase within one week ( $< 5\%$ , Fig. 3B), which implies a very slow sedimentation of all formulations within 7 days [37,38]. Fig. 3C shows that the particle size of the three nanosuspensions increased, steady, and then downward trend as dilution was increased. The maximum increase of particle size was less than  $100\text{ nm}$  for all the formulations, indicating that the three nanosuspensions had relatively good dilution stability [34]. Fig. 3D shows that the particle size of the three nanosuspensions increased immediately after adding plasma. It can be speculated that protein adsorption on the surface of nanoparticles may have occurred. As shown in Fig. 3E, the results of Coomassie brilliant blue test confirmed that protein adsorption occurred when the nanosuspensions were incubated with plasma, which results indicated that the three nanosuspensions may be easily recognized by opsins in plasma after entering the blood circulation, which is beneficial to the accumulation of nanosuspensions into the monocyte-macrophage system (MPS) [39,40]. The particle size of the three nanosuspensions remained mostly unchanged with the prolongation of incubation time as shown in Fig. 3D, which indicated that the three nanosuspensions had good stability in plasma after absorption of protein [41]. Also, the results of the hemolysis experiment indicated that the three nanosuspensions had good blood compatibility in the range of  $50$ – $400\ \mu\text{g/mL}$ . The above results implied that the three nanosuspensions have good stability and can be safely used for intravenous administration within appropriate concentration range [42,43].

Solubilization of insoluble drugs is one of the key advantages of nanosuspensions. Fig. 3F shows that the cumulative dissolution of HCPT and QUR from the nanosuspensions were much larger than those of raw HCPT and QUR within the same time frame, which is

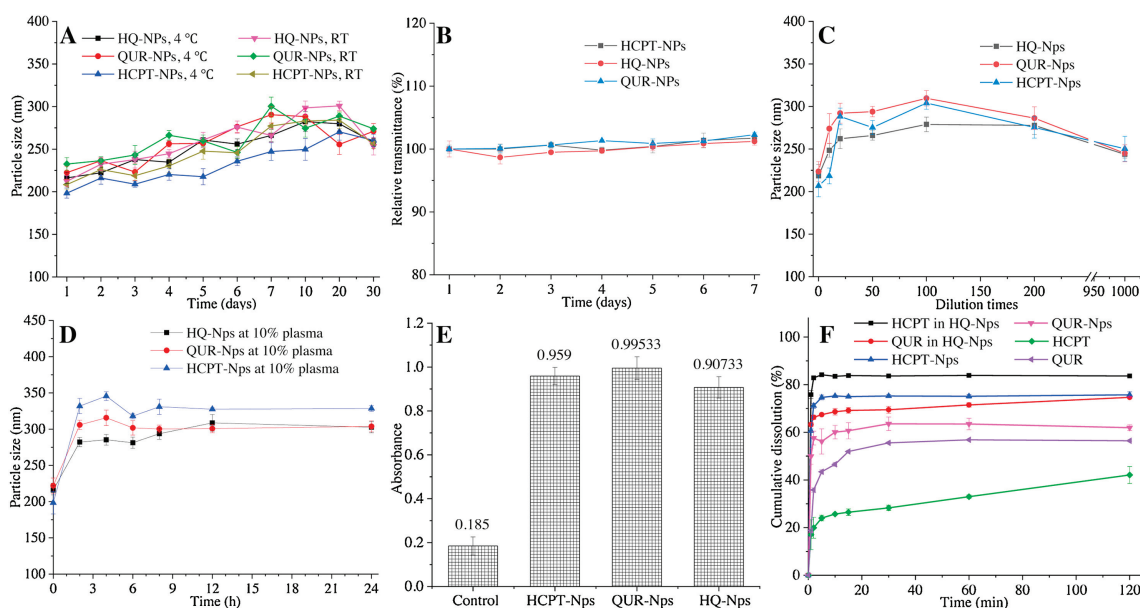


**Fig. 3.** (A) The storage stability of nanosuspensions at  $4^{\circ}\text{C}$  and room temperature within 30 days, (B) the kinetics stability at room temperature within 7 days, (C) the dilution stability, (D) the stability of nanosuspensions in plasma, (E) the results of protein adsorption test, and (F) the drug dissolution curve of three nanosuspensions.

due to the increase of specific surface area and the change of crystal form in the nanosuspensions [23,44]. The dissolution rate of HCPT in HQ-NPs was significantly higher than that in HCPT-NPs because the incorporation of QUR significantly changed the crystal state of HCPT and that the binding affinity between HCPT and QUR was less than that between two HCPT molecules. In addition, the more rapid dissolution rate of QUR in HQ-NPs than that in QUR-NPs could be attributed to the amorphous state of QUR in HQ-NPs.

To study the anti-resistance of HQ-NPs, *in vitro* cytotoxicity to sensitive and drug resistant cells were investigated. The inhibition of QUR-NPs on HepG2 cells and A549/PTX cells was the weakest in all groups as seen from Figs. 4A and B, which indicated that the anti-tumor efficiency of QUR was weaker than that of HCPT. The inhibition effect of HCPT-NPs on sensitive cells HepG2 was like that of HQ-NPs and stronger than that of HQ-solutions. However, the inhibition effect of HCPT-NPs on drug-resistant cells was far weaker than that of HQ-NPs, even weaker than that of HQ-solutions. These results indicate that the combination of QUR and HCPT can significantly increase the inhibition effect of HCPT on the proliferation of drug-resistant cells [44]. So, it can be inferred that QUR may increase the uptake of HQ-NPs by A549/PTX cells by inhibiting P-gp [45]. Excitedly, the results of cell uptake tests show that the uptake rates of HQ-NPs ( $23.48\% \pm 2.03\%$  and  $38.08\% \pm 1.71\%$ , respectively) by A549/PTX cells were indeed significantly higher than those of HCPT-NPs ( $19.54\% \pm 0.17\%$  and  $27.18\% \pm 0.64\%$ , respectively) after co-culture for 0.5 h and 2 h (Table S2 in Supporting information). It can be seen from the results that the increase of the cell uptake rate of HQ-NPs was about twice as much as that of HCPT-NPs from 0.5 h to 2 h (Fig. S5 in Supporting information). These results explained why the inhibition effect of HQ-NPs on A549/PTX was stronger than that of HCPT-NPs.

In this study, the evaluation of *in vivo* tissue distribution, anti-tumor, immunomodulatory, and biosafety effects were also carried out in H22 tumor xenograft mice for HQ-solution, QUR-NPs, HCPT-NPs, and HQ-NPs. As shown in Fig. 4C, the tumor grew rapidly in the saline group and the tumor volume was significantly larger than that in other groups after 14 days. In the administration groups, the tumor volume in the QUR-NPs group was largest, the tumor volume of the HQ-solution group was in the middle, those of HCPT-NPs and HQ-NPs were very small. These results indicate that the anti-tumor effect of HCPT-NPs and HQ-NPs were strongest,

**Table 2**

The SR, TI and SI after administration of different drug formulations for 14 days.

Group	SR	SI (mg/g)	TI (mg/g)
Saline	100%	$6.50 \pm 0.82$	$2.52 \pm 0.67$
HCPT-NPs	50%	$4.31 \pm 0.29^{**}$	$1.38 \pm 0.09^{***}$
QUR-NPs	100%	$7.51 \pm 0.91^{\Delta\Delta\Delta}$	$3.43 \pm 0.70^{\Delta\Delta\Delta}$
HQ-NPs	100%	$7.25 \pm 0.82^{\Delta\Delta\Delta\Diamond\Diamond}$	$3.07 \pm 0.55^{\Delta\Delta\Diamond}$
HQ-solution	85%	$3.21 \pm 0.74^{**}$	$1.40 \pm 0.36^{***}$

\* Represents comparison with the saline group,  $\Delta$  represents comparison with the HQ-solution group,  $\Diamond$  represents comparison with the HCPT-NPs group. One symbol implies  $P < 0.05$ , two symbols imply  $P < 0.01$ , and three symbols imply  $P < 0.001$ .

which may be attributed to the following several reasons: 1) The anti-tumor efficiency of QUR was very weak as shown in cytotoxicity *in vitro*; 2) The accumulation of HCPT-NPs and HQ-NPs in tumor tissue was higher than that of HQ-solution at each time point as confirmed by tissue distribution *in vivo* (Fig. S6 in Supporting information); 3) Most of the HCPT in HQ-solution exists as carboxylates, which greatly reduced the anti-tumor activity of HCPT, was not conducive to cell uptake, and also was easily cleared by the body [16,46]. Additionally, there was no significant difference in tumor volume and inhibition rate (Fig. S7 in Supporting information) between HQ-NPs group and HCPT-NPs group, indicating that the anti-tumor effects of the two suspensions was similar. Considering that the concentration of HCPT in HQ-NPs was only 3/5 of that in HCPT-NPs, however, the accumulation of HCPT in HCPT-NPs and HQ-NPs was close in tumor (Fig. S6), it can be inferred that QUR promoted the uptake of HCPT by tumor cells and may have a synergistic effect with HCPT in HQ-NPs as confirmed by the *in vitro* cell uptake and cytotoxicity tests.

Fig. 4D shows the change of mouse's body weight after intermittent administration for 14 days. The body weight of mice in the saline group, QUR-NPs group, and HQ-solution group showed an increasing trend, which may be attributed to the normal growth of mice and the increase of tumor volume [47]. The body weight of mice in the HQ-NPs group was well controlled, which may be due to inhibition of tumor volume. However, the body weight of mice in the HCPT-NPs group decreased significantly, which may be attributed to the serious side effects caused by a high dose of HCPT.

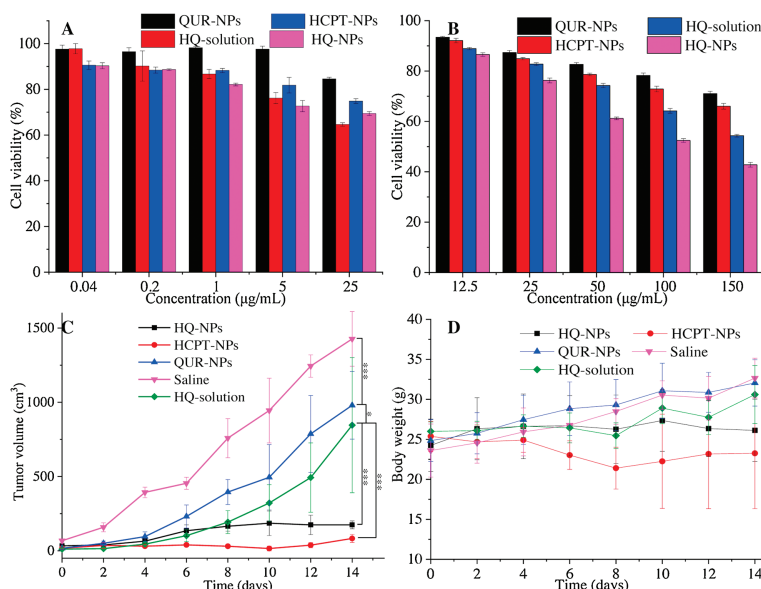


**Fig. 4.** The viability of HepG2 cells (A) and A549/PTX cells (B) treated with different formulations for 24 h. The changes in tumor volume (C) and body weight (D) after administration ( $n = 14$ ).

Table 2 shows the survival rate (SR), thymus index (TI), and spleen index (SI) in each group. From comparison of the survival rate of mice in HQ-solution and HQ-NPs groups, it can be inferred that the systemic toxicity of HCPT can be reduced by nanosuspensions. When comparing the survival rate of mice in HCPT-NPs and HQ-NPs groups, the combination therapy of HCPT and QUR also reduced the systemic toxicity of HCPT. These results can also be confirmed by H&E staining images in immunohistochemical analysis as shown in Fig. S8 (Supporting information). In H&E staining images of HCPT-NPs group, there were obvious cell fragments and vacuoles (black arrow) in the heart, liver, and kidney tissue sections of mice, but there was no significant change in heart, liver, spleen, lung, and kidney tissue sections of mice in HQ-NPs groups, which further indicated that QUR could reduce the systemic toxicity of HCPT.

To study the immunomodulatory effect of QUR, the thymus and spleen indexes of mice were calculated, and the results are shown in Table 2. As shown in Table 2, the thymus and spleen indexes in HQ-solution and HCPT-NPs groups were significantly lower than those in the normal saline group ( $P < 0.001$  and  $P < 0.01$ ). These results indicated that HQ-solution and HCPT-NPs had a certain inhibition effect on thymus and spleen, which may be attributed to the toxicity of HCPT. However, the thymus and spleen indexes of QUR-NPs and HQ-NPs groups were significantly higher than those of the HQ-solution group ( $P < 0.001$ ,  $P < 0.01$  or  $P < 0.001$ ), and slightly higher than those of saline group. These results indicated that QUR had a protective effect on immune organs.

In this paper, a new amphiphilic triblock copolymer PEG-(PBLA)<sub>2</sub> was synthesized as a stabilizer, and a hybrid nanosuspensions (HQ-NPs) was manufactured by the microprecipitation-high pressure homogenization method with HCPT-NPs and QUR-NPs as control. The three nanosuspensions had the size of about 200 nm, different morphologies, good stability, and blood compatibility. DSC and XRD results proved that the crystal phase transition of HCPT and QUR may occur during the formation of nanosuspensions, and their heterozygosity in HQ-NPs changed their physical state, which further influences the dissolution rates of HCPT and QUR in different formulations. Excitedly, the MD data of the two drugs explain these results. The results of cytotoxicity test and the drug uptake assay showed QUR in HQ-NPs could increase anti-tumor effect by increasing the uptake of HCPT by A549/PTX cells. In H22 tumor-bearing mice, HQ-NPs enhanced the accumulation HCPT in tumor tissue, and showed strong activity to inhibit tumor growth and good biological safety which was verified by the changes in tumor volume and body weight, survival rate, immune organ index, and H&E staining image of tissue. In conclusion, HQ-NPs showed strong anti-tumor activity *in vivo* and *in vitro*, and significantly reduced the side effects on normal tissues, indicating that HQ-NPs had a good synergistic effect and attenuated toxicity. HQ-NPs, therefore, can offer good potential for the development of a safe, effective, and novel dosage form of HCPT.

#### Declaration of competing interest

The authors report no declarations of interest

#### Acknowledgments

This work was supported by Leading Talents Program of Zhongyuan Science and Technology Innovation (No. 204200510022), Program for Innovative Research Team (in Science

and Technology) in University of Henan Province (No. 21IRTSTHN026), Henan Provincial Key Research-Development and Special Project For Promotion (Nos. 192102310030, 202102310483); Kaifeng Science and Technology Development Plan Project and the Key Project of Science (Nos. 1903034, 1908006), the Key Project of Science and Technology Research funded by the Henan Provincial Department of Education (No. 19A350001). We also thank Clairissa Dela Cruz Corpstein (College of Pharmacy, Purdue University) for her linguistic assistance during the preparation and revision of this manuscript.

#### Appendix A. Supplementary data

Supplementary material related to this article can be found, in the online version, at doi:<https://doi.org/10.1016/j.ccl.2021.03.049>.

#### References

- [1] E. Dubikovskaya, S. Thorne, T. Pillow, C. Contag, P. Wender, Proc. Natl. Acad. Sci. U. S. A. 105 (2008) 12128–12133.
- [2] C.X. Yang, L. Xing, X. Chang, et al., Mol. Pharm. 17 (2020) 1300–1309.
- [3] M.R. Salehan, H.R. Morse, Br. J. Biomed. Sci. 70 (2013) 31–40.
- [4] Y. Sun, W. Ma, Y. Yang, et al., Asian J. Pharm. Sci. 14 (2019) 581–594.
- [5] Y. Zhang, F. Wang, M. Li, et al., Adv. Sci. 5 (2018) 1800811.
- [6] L. Sun, D. Wang, Y. Chen, et al., Biomaterials 133 (2017) 219–228.
- [7] T.J. Curiel, Drug Resist. Updat. 15 (2012) 106–113.
- [8] Y. Liu, Y.J. Kim, N. Siriwon, et al., Biotechnol. Bioeng. 115 (2018) 1403–1415.
- [9] W. Zhang, J. Shen, H. Su, et al., ACS Appl. Mater. Interfaces 8 (2016) 13332–13340.
- [10] Q. Huo, J. Zhu, Y. Niu, et al., Int. J. Nanomedicine 12 (2017) 8631–8647.
- [11] J. Wang, F. Wang, F. Li, et al., J. Mater. Chem. B Mater. Biol. Med. 4 (2016) 2954–2962.
- [12] H. Wang, L. Zhou, K. Xie, et al., Theranostics 8 (2018) 3949–3963.
- [13] W. Han, L. Shi, B. Xie, et al., ACS Appl. Mater. Interfaces 12 (2020) 1707–1720.
- [14] X.H. Pu, J. Sun, Y.M. Qin, et al., Curr. Nanosci. 8 (2012) 762–766.
- [15] L. Yang, J. Hong, J. Di, et al., Int. J. Nanomedicine 12 (2017) 3681–3695.
- [16] X.H. Pu, J. Sun, J.H. Han, et al., J. Nanopart. Res. 15 (2013) 2043–2055.
- [17] Y. Qiao, Y. Cao, K. Yu, L. Zong, X. Pu, Int. J. Pharm. 589 (2020) 119830.
- [18] H.B. Hyun, J.Y. Moon, S.K. Cho, Molecules 23 (2018) 209.
- [19] Z. Zhang, S. Xu, Y. Wang, et al., J. Colloid Interface Sci. 509 (2018) 47–57.
- [20] A. Primikyri, M.V. Chatziathanasiadou, E. Karali, et al., ACS Chem. Biol. 9 (2014) 2737.
- [21] B. Cote, L.J. Carlson, D.A. Rao, A.W.G. Alani, J. Control. Release 213 (2015) 128–133.
- [22] X. Wang, Y. Chen, F.Z. Dahmani, et al., Biomaterials 35 (2014) 7654–7665.
- [23] M. Li, Y. Chen, L. Yin, et al., Sci. Adv. Mater. 9 (2017) 1713–1723.
- [24] X.H. Pu, J. Sun, M. Li, Z.G. He, Curr. Nanosci. 5 (2009) 417–427.
- [25] J. Li, Q. Fu, X. Liu, M. Li, Y. Wang, Arch. Pharm. Res. 39 (2016) 202–212.
- [26] H. Zhang, F. Teng, P. Wang, et al., Int. J. Pharm. 477 (2014) 88–95.
- [27] D. An, J. Fu, Z. Xie, et al., J. Mater. Chem. B: Mater. Biol. Med. 8 (2020) 7076–7120.
- [28] Q. Liu, Z. Xie, M. Qiu, et al., Adv. Sci. 7 (2020) 2001191.
- [29] M. Qiu, D. Zhu, L. Yan, et al., J. Phys. Chem. C 120 (2016) 22757–22765.
- [30] M. Qiu, R.G. Brandt, Y. Niu, et al., J. Phys. Chem. C 119 (2015) 8501–8511.
- [31] Q. Peng, J. Liu, T. Zhang, et al., Biomacromolecules 20 (2019) 1789–1797.
- [32] Y. Lu, Y. Lv, T. Li, Adv. Drug Deliv. Rev. 143 (2019) 115–133.
- [33] X. Tian, L. Zhang, M. Yang, et al., WIREs Nanomed. Nanobiotech. 10 (2018) e1476.
- [34] L. Zong, X. Li, H. Wang, et al., Int. J. Pharm. 531 (2017) 108–117.
- [35] Y. Kojo, S. Matsunaga, H. Suzuki, et al., Eur. J. Pharm. Sci. 97 (2017) 55–61.
- [36] X. Zhang, T. Zhang, Y. Lan, B. Wu, Z. Shi, AAPS PharmSciTech 17 (2016) 400–408.
- [37] G.Y. Zhu, B.Y. Lu, T.X. Zhang, et al., Nanomed. 13 (2018) 1093–1106.
- [38] B.Y. Lu, G.Y. Zhu, C.H. Yu, et al., Nano Res. 14 (2020) 185–190.
- [39] Q. Yuan, Y. Wang, R. Song, et al., Front. Pharmacol. 10 (2019) 225.
- [40] H. Gao, Q. He, Expert Opin. Drug Deliv. 11 (2014) 409–420.
- [41] X. Pu, L. Zhao, J. Li, et al., Acta Biomater. 88 (2019) 357–369.
- [42] L. Mei, Y. Liu, H. Zhang, et al., ACS Appl. Mater. Interfaces 8 (2016) 9577–9589.
- [43] H.B. Ruttala, T. Ramasamy, B.S. Shin, et al., Int. J. Pharm. 519 (2017) 11–21.
- [44] Y. Cao, Z. Wei, M. Li, et al., Curr. Cancer Drug Targets 19 (2019) 338–347.
- [45] D.R. Reddy, A. Khurana, S. Bale, et al., Springerplus 5 (2016) 1618.
- [46] M. Han, X. Liu, Y. Guo, Y. Wang, X. Wang, Int. J. Pharm. 455 (2013) 85–92.
- [47] L. Yang, J. Jiang, J. Hong, et al., J. Biomed. Nanotechnol. 11 (2015) 711–721.